Available online at www.sciencedirect.com
SCIENCE DIRECT®
Virology 344 (2006) 340 – 353
VIROLOGY
www.elsevier.com/locate/yviro

Apparent elimination of EIAV ancestral species in a long-term inapparent carrier

Jodi K. Craigo [a], Timothy J. Sturgeon [a], Sheila J. Cook [b], Charles J. Issel [b], Caroline Leroux [a,1], Ronald C. Montelaro [a,*]

[a] Department of Molecular Genetics and Biochemistry, University of Pittsburgh School of Medicine, Pittsburgh, PA 15261, USA
[b] Department of Veterinary Science, Gluck Equine Research Center, University of Kentucky, Lexington, KY 40546, USA

Received 15 June 2005; returned to author for revision 10 August 2005; accepted 7 September 2005
Available online 13 October 2005

Abstract

Equine infectious anemia virus (EIAV) envelope variation produces newly dominant quasispecies with each sequential disease cycle; new populations arise, and previous plasma quasispecies, including the original inoculum, become undetectable. The question remains whether these ancestral variants exist in tissue reservoirs or if the immune system eliminates quasispecies from persistent infections. To examine this, an EIAV long-term inapparent carrier was immune suppressed with dexamethasone. Immune suppression resulted in increased plasma viral loads by approximately 10^4 fold. Characterization of pre- and post-immune suppression populations demonstrated continual envelope evolution and revealed novel quasispecies distinct from defined populations from previous disease stages. Analysis of the tissue and plasma populations post-immune suppression indicated the original infectious inoculum and early populations were undetectable. Therefore, the host immune system apparently eliminated a diverse array of antigenic variants, but viral persistence was maintained by relentless evolution of new envelope populations from tissue reservoirs in response to ongoing immune pressures.

Keywords: EIAV; Lentiviral evolution; Envelope variation; Reservoir populations; Lentiviral latency; Ancestral populations

Introduction

Natural and experimental infection of equids with equine infectious anemia virus (EIAV) results in a rapid and dynamic disease process that differs markedly from the slowly progressive degenerative diseases associated with other lentiviral infections including HIV-1 infection of humans. EIA disease is characterized by three distinct stages: acute, chronic, and long-term asymptomatic (Clements et al., 1994; Montelaro et al., 1993; Oaks et al., 1998). Acute disease is typically observed within 3 to 4 weeks post-infection and is associated with high levels of viremia and clinical signs of disease including fever, diarrhea, lethargy, edema, thrombocytopenia, and anemia. Chronic EIA, characterized by repeated cycles of disease and associated waves of viremia, lasts approximately 8 to 12 months post-infection. EIA disease cycles occur at irregular intervals, separated by weeks or months, with an average of six to eight disease episodes within the first year post-infection. At this time, most infected horses become asymptomatic for EIA indefinitely, presumably due to the development of enduring protective host immunity. These inapparent carriers, however, remain infected for life with the maintenance of markedly different subclinical levels of steady state virus replication (Harrold et al., 2000; Leroux et al., 2001). Thus, EIAV offers a unique model for characterizing natural immunologic control of lentivirus replication and disease and for elucidating the nature and role of viral variation in persistence and pathogenesis.

Studies of EIAV variation during persistent infection in experimentally infected equids have clearly identified dynamic changes in envelope sequences that alter viral antigenic properties, evidently as a result of immune selection (Leroux et al., 1997b, 2001; Lichtenstein et al., 1996). The predominant site of EIAV variation during persistent infection is the gp90 surface envelope glycoprotein, and the pattern of gp90

* Corresponding author. Fax: +1 412 383 8859.
E-mail address: rmont@pitt.edu (R.C. Montelaro).
[1] Present address: UMR 754 INRA-Université Claude Bernard Lyon I-Ecole Nationale Vétérinaire de Lyon, IFR 128.

0042-6822/$ - see front matter © 2005 Elsevier Inc. All rights reserved.
doi:10.1016/j.virol.2005.09.006

nucleotide and amino acid variation has been analyzed to define distinct conserved and variable protein domains (Leroux et al., 1997b) as observed with other animal and human lentiviruses (Greene et al., 1993; Leroux et al., 1997a; Simmonds et al., 1990; Starcich et al., 1986; Suarez and Whetstone, 1995). These patterns of EIAV envelope variation and defined conserved and variable envelope domains have been confirmed by others (Zheng et al., 1997a, 1997b). Variation of the EIAV envelope gene has therefore served as a distinct marker for analysis of viral population evolution.

Previous studies from our laboratory have demonstrated that the viral populations associated with the cyclic disease episodes of chronic EIA are distinct genomic and antigenic variants (Leroux et al., 1997b, 2001; Payne et al., 1987). Detailed molecular characterization of EIAV envelope variation during sequential disease cycles in experimentally infected ponies revealed the presence of distinct EIAV envelope variants with each wave of viremia (Leroux et al., 1997b). Examination of inapparent stage viral populations from the plasma of the same ponies indicated that evolution of the viral quasispecies is continuous, even with relatively low levels of detectable virus replication in the periphery or tissues (Leroux et al., 2001). These results suggest that, even in the absence of detectable plasma virus, viral populations, most likely in tissue reservoirs, continue to replicate and evolve, seeding the plasma with new viral quasispecies.

Tissue reservoirs of lentiviral populations have been designated not only as active sites of replication, but also as reservoirs for latent viral genomes (Blankson et al., 2002; Chun et al., 1997). The development of viral reservoirs contributes to the extraordinary level of persistence and in some instances pathogenesis associated with lentiviral infections (Finzi et al., 1999; Persaud et al., 2003). Tissue reservoirs can harbor a stable pool of viral populations undergoing cryptic low levels of replication or contain a latent viral population such as observed with HIV-1 found in resting memory CD4+ T cells (Han et al., 2004; Lassen et al., 2004). In both cases, tissue reservoirs theoretically can provide a stable archive of quasispecies reflecting the entire history of the viral infection. Whether early or initial viral quasispecies are completely eliminated from the archive of lentiviral reservoir populations has not been established.

An interesting observation from our previous studies of chronic and inapparent stage viral isolate evolution is that there appeared to be a consistent loss of ancestor populations. The departure of ancestral populations was concurrent with the appearance of new Env quasispecies, suggesting effective immune suppression or elimination of the prior actively replicating quasispecies. These snapshots of viral populations were all taken from isolates circulating in the plasma. Thus, it is possible that infecting and transient quasispecies may continue to exist in tissue reservoirs as latent or low replicating provirus in infected monocytes and macrophage. Severe immune suppression of EIAV-infected equids through administration of the glucocorticoid dexamethasone has been previously demonstrated to suppress the host immune system and induce the recrudescence of viral replication and clinical EIA (Craigo et al., 2002; Kono et al., 1976; Tumas et al., 1994). Removal of the immune control of the latent EIAV reservoirs theoretically frees viral replication that can enable detection of not only minor populations, but also of the archived ancestral populations. Therefore, to determine whether early viral populations remained within the infected host, we immune suppressed a long-term EIAV inapparent carrier (30 months) from which plasma viral evolution had been characterized in detail (Leroux et al., 1997b, 2001). Viral populations detected and analyzed before and during immune suppression, in both tissues and plasma, for the first time indicated an effective elimination of ancestor viral quasispecies from infected equids, suggesting that the host immune system is able to effectively eliminate persistent infection by a range of type-specific quasispecies.

Results

Clinical and virologic profile during $EIAV_{PV}$ infection and subsequent immune suppression

Previous studies from our laboratory extensively characterized envelope variation in long-term inapparent carrier ponies experimentally infected with our pathogenic strain, $EIAV_{PV}$ (Leroux et al., 1997b, 2001). The four ponies were each classified as either “progressor” or “nonprogressor” based on the disease process experienced by each individual animal (Leroux et al., 2001). Pony #567, a progressor pony, experienced six febrile episodes accompanied by high viral loads (10^6–10^9 RNA copies/ml plasma) over the initial 750-day observation period (Fig. 1). Following the sixth fever, pony #567 entered the inapparent stage of EIA and was asymptomatic throughout the rest of the 3.5-year observation period but maintained low levels of viral replication which averaged approximately 10^3 RNA copies/ml plasma (Fig. 1). Pony #567 viral envelope characterization exhibited elevated levels of gp90 variation (amino acid divergence = 7.44 ± 0.48%) and produced the highest number of evolving viral populations (32 detected populations from inoculum to final inapparent analysis) as compared to the other experimentally infected ponies (Leroux et al., 2001). While the viral quasispecies in pony #567 continued to evolve new variant species, viral quasispecies which had appeared in the early stages of disease, including the original infectious inoculum, were no longer detectable in plasma.

To explore all the viral populations persisting in pony #567, we chemically immune suppressed this pony for a 14-day period to release immunologic restraint of all existing viral quasispecies and allow free replication of virus from tissue reservoirs. Prior to immune suppression, pony #567 demonstrated no clinical signs of EIA disease and low to moderate viral loads which averaged approximately 10^3 RNA copies/ml plasma. Immune suppression was carried out through daily I.M. injections of 0.11 mg/kg of dexamethasone (1224 D.P.I. to 1237 D.P.I.). Pony #567 was monitored daily for adverse affects of the drug. Recrudescence of viral species as well as disease was contingent on thorough depression of the immune system. Successful suppression of pony #567 immune system

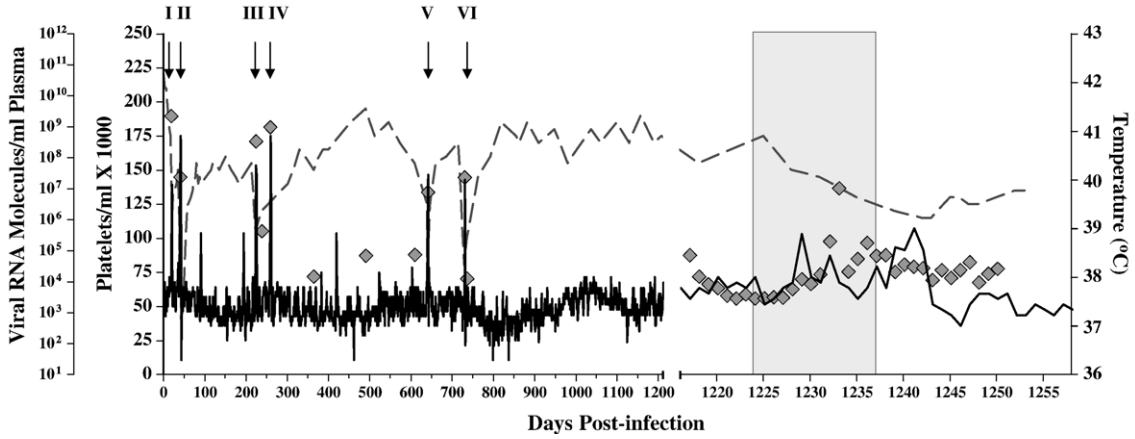

Fig. 1. Clinical and virological profile of experimentally infected and immune suppressed pony #567. Pony #567 was experimentally infected with 10^3 $TCID_{50}$ of the biological clone $EIAV_{PV}$. Rectal temperatures (—, right *y* axis) and platelet counts (----, 1st left *y* axis) were followed daily for up to 1250 days (*x* axis) after inoculation and during immune suppression. Quantitation of the virus load (♦, 2nd left *y* axis) was performed on viral RNA extracted from plasma at periodic time points throughout the initial infection, fever episodes, and asymptomatic stages and daily during immune suppression observation period. The period of immune suppression is designated by a shaded box. Febrile episodes were defined by a rectal temperature above 39 °C in conjunction with a reduction in the number of platelets below 100,000/μl of whole blood and other clinical signs of EIA disease. I, II, III, IV, V, and VI (↓) indicate fever episodes.

was consequently monitored utilizing both in vivo delayed-type hypersensitivity (DTH) analysis and in vitro fluorescence-activated cell sorting (FACS) analysis of CD4+ and CD8+ cells (Fig. 2). DTH assays were utilized at multiple time points throughout the dexamethasone treatment and revealed a marked decrease in reactivity during drug treatment, the DTH ratio decreasing from 2.5 prior to treatment to 1.25 on day 11 of treatment. Further verification of the efficacy of immune suppression was performed concurrently through FACS staining of CD4+ and CD8+ PBMC taken from the pony during the immune suppression regimen (Fig. 2). FACS analysis also exhibited suppression of the immune system, with CD4+ cells decreasing from 28% to 9% and CD8+ cells decreasing from 18% to 2%. The results of both the DTH and FACS analysis clearly indicated successful immune suppression by the end of the 14-day dexamethasone treatment while also demonstrating quick recovery of the immune system following removal of drug treatment. The animal developed no clinical signs of EIA during the extensive 14-day immune suppression period. Platelet levels showed minor decreases that are commonly observed with increased viral replication but never dropped to the point of the thrombocytopenia associated with EIA (Fig. 1). Likewise, the daily rectal temperature of #567 demonstrated fluctuations, however, the peaks in temperature never crossed the threshold of 39 °C that is indicative of EIA disease. Viral replication increased from 10^3 to 10^7 RNA copies/ml plasma during immune suppression, peaking at 10^7 RNA copies/ml plasma on day 10 of treatment but returned within 6 days to moderate levels of 10^4 RNA copies/ml plasma prior to cessation of treatment.

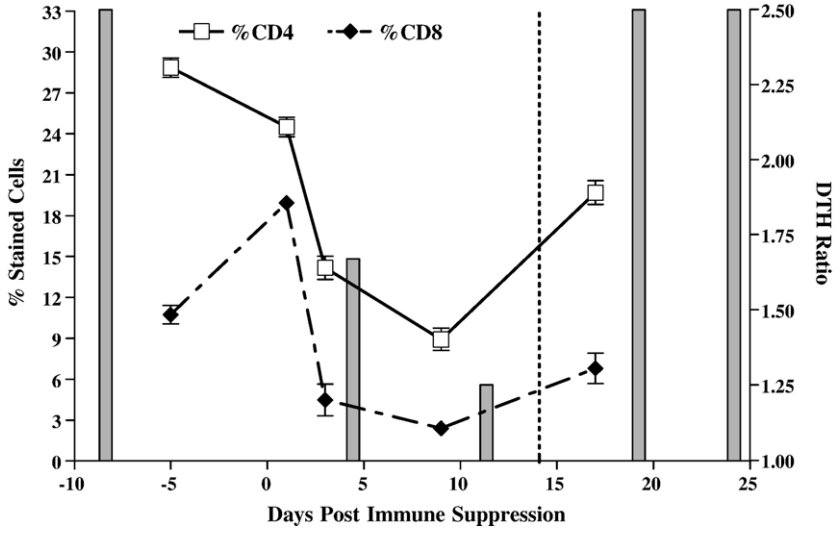

Fig. 2. Verification of immune suppression via both in vivo and in vitro analyses. To measure in vivo the effects of dexamethasone suppression of the immune system, a delayed-type hypersensitivity assay was performed as described in Materials and methods (shaded bars, right *y* axis). PBMC samples were assayed in in vitro FACS assays (left *y* axis) as described in Materials and methods to confirm the effect of the dexamethasone on the immune suppression. □, CD4+; ♦, CD8+; ----, indicates the end of drug treatment.

Population analysis of #567 viral populations before and during immune suppression

Previous studies from our laboratory (Leroux et al., 1997a, 2001; Lichtenstein et al., 1996; Payne et al., 1989) and others (Zheng et al., 1997a, 1997b) indicate that EIAV envelope variation during persistent infection is localized to specific segments of the gp90 surface glycoprotein, with relatively minor variation observed in the gp45 transmembrane protein. Therefore, for this study, we focused on the highest region of variability within the gp90 envelope protein, the third variable region (V3) through the seventh variable region (V7). Since there was a 500-day period between the last population analysis and the start of immune suppression, we initially determined the EIAV population immediately prior to the immune suppression (Leroux et al., 2001). EIAV quasispecies were examined therefore immediately prior to and during the period of immune suppression. EIAV envelope sequences were determined using viral RNA recovered from pelleted plasma virus or lymph node tissue virus prior to (1207 D.P.I.-tissue/1219 D.P.I-plasma) and during (1234 D.P.I.-plasma/1239 D.P.I.-tissue) immune suppression (referred to as post-immune suppression). A total of 85 clones from the immune suppression period were subjected to sequence analysis in addition to a combined analysis of 52 additional febrile isolate clones from previous studies for a combined total of 137 clones analyzed for this population study.

Nature of pony #567 viral quasispecies amino acid sequence changes

The principal goal of the current study was to examine whether the initial infecting viral quasispecies or early febrile virus populations remained in minor populations and/or in tissue reservoirs after long-term infection. Once nucleotide sequencing of the V3–V7 regions of the envelope was completed, the deduced amino acid sequences were visually inspected to determine the phenotype of the viral quasispecies. The pre-immune and post-immune suppression viral quasispecies as compared to $EIAV_{PV}$ and febrile isolates demonstrated a wide array of alterations including insertions, deletions, and point mutations of amino acids within the defined gp90 variable domains of the envelope. As observed in previous studies, the frequent modification of viral envelope potential *N*-glycosylation sites was the most conspicuous change in addition to the insertion of additional asparagines into the already asparagine-rich segment of the V7 region (Craigo et al., 2002; Leroux et al., 1997b, 2001). Ultimately, visual analysis of the viral population revealed that there was no evidence of $EIAV_{PV}$ or predecessor quasispecies in any of the populations sampled.

To further characterize the sequences derived during the immune suppression of pony #567, we compared the temporal generation of variant amino acid sequences of the emergent envelope species. Due to the number of sequences involved in these analyses and the size of the figure they would create, the actual sequences are not pictured, but the GenBank accession numbers are provided. To demonstrate the extensive variation that occurred throughout the current study period in a succinct manner, we used the level of variation of the highest variable region of the envelope, the V3 region, as a marker of evolution (Fig. 3). As previously observed, only two of the sequenced clones had a V3 sequence identical to $EIAV_{PV}$ by the first fever (Leroux et al., 2001). At the time of the second fever, all clones were different from $EIAV_{PV}$, and none of the species present during the first fever was apparent. In general, during the chronic stage of disease, new envelope quasispecies that typically were present only at a single disease cycle rapidly replaced the previous population with no further evidence of the inoculum $EIAV_{PV}$ species. The current observation period or inapparent phase of disease revealed similar patterns of evolution. The pre-immune suppression plasma and tissue populations all demonstrated entirely new V3 regions that do not indicate overlapping populations even with each other while sampled only days apart prior to drug treatment. The post-immune suppression quasispecies reveal for the first time the apparent reappearance of previously demonstrated signatures in the V3 region. However, the overlap of populations is with the pre-immune suppression tissue and plasma quasispecies. The fact that the immune suppressive drug treatment would allow replication of previous viral quasispecies also may explain the overlapping V3 signatures. While these variants do appear to reflect the influence of the immune suppression through recurring species sampling, this time point also exhibited the emergence of new V3 regions (7 completely novel species) in the tissue and plasma isolates combined.

Verification of the lymph node tissue as a viral population reservoir

To confirm that the lymph node was serving as a reservoir of viral quasispecies, nucleotide sequences were examined. The analyses were performed solely on the viral isolates from the tissues and plasma pre- and post-immune suppression. The sequences spanning the V3 to V7 region of the *env* gp90 gene were aligned to the sequence of the original infecting inoculum, $EIAV_{PV}$. Our first goal was to verify the lymph node tissue as a reservoir for viral populations. One would expect a reservoir population to have higher levels of genetic diversity as compared to a contemporous or actively replicating population, while additionally having a lower level of divergence (Nickle et al., 2003a, 2003b). A contemporous population would have increased divergence compared to a reservoir population due to the higher levels of evolution that occurs through misincorporation of nucleotides by the viral reverse transcriptase that is associated with active replication (Bakhanashvili and Hizi, 1993; Preston et al., 1988; Roberts et al., 1988). Likewise, the diversity within a reservoir population, which serially samples and archives viral species over long periods of time, would be greater than that of a contemporous population. Therefore, to determine whether the lymph nodes served as a tissue reservoir of viral populations, we compared the diversity within the quasispecies between the lymph node and plasma as well as the divergence of the lymph node and plasma populations from the inoculating strain ($EIAV_{PV}$) (Fig. 4). As summarized in Fig. 4, prior to

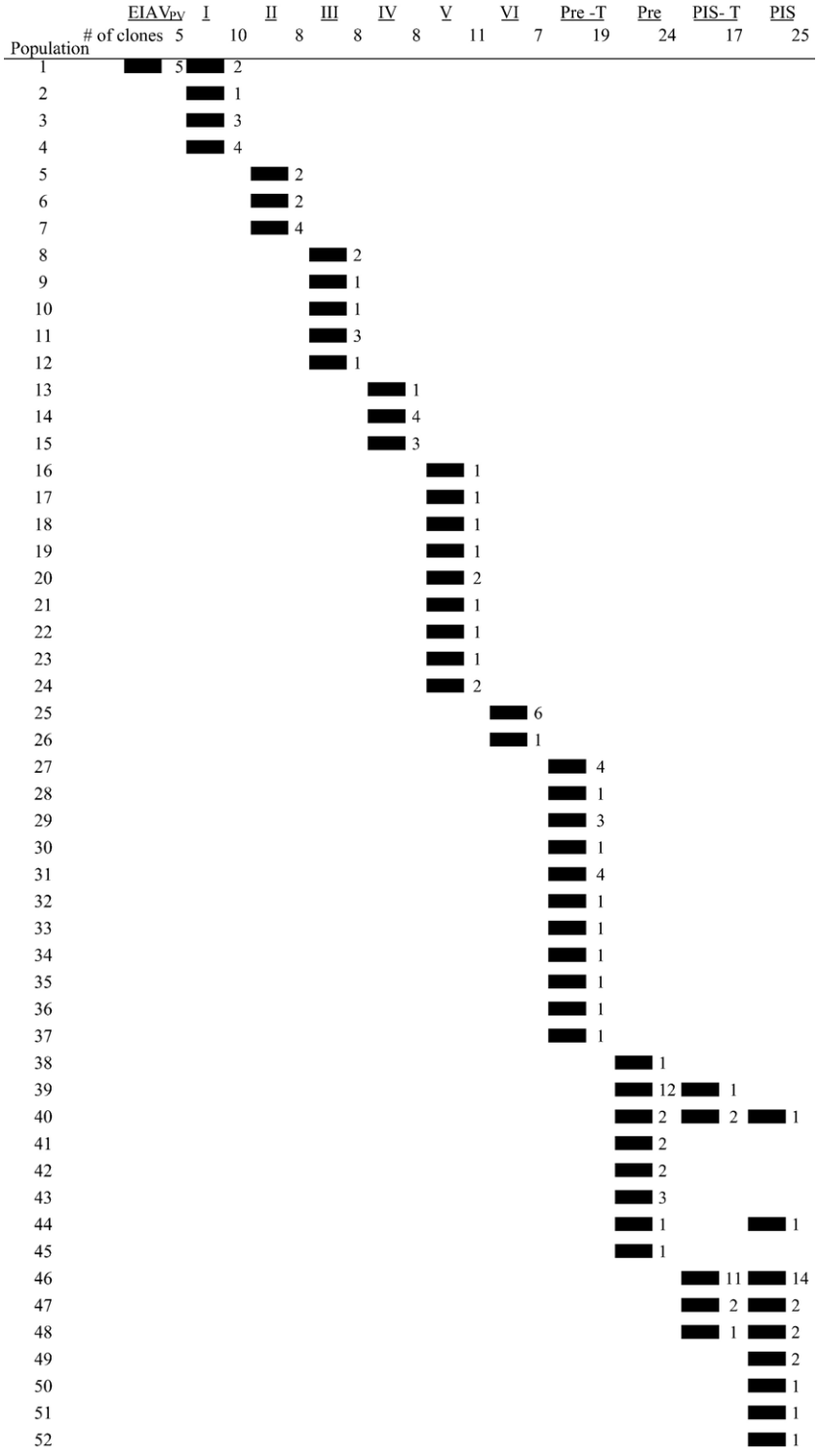

Fig. 3. Temporal evolution of gp90 V3 envelope species in pony #567. The figure represents the temporal evolution of the gp90 V3 envelope variable domain of longitudinal viral populations in pony #567. Each deduced amino acid sequence of gp90 variable regions V3 is depicted as species 1 through 52. The number of clones containing each specific genetic species is listed in the column after the species symbol, with the total number of clones analyzed indicated at the top of the figure within that same column. Viral plasma species were determined for the fever episodes (I, II, III, IV, V, and VI) and immune suppression phase of the study. Each bar represents a species present during the indicated time period (i.e., the inoculum contained a single species). Pre-T, pre-immune suppression tissue; Pre, pre-immune suppression plasma; PIS-T, post-immune suppression tissue; PIS, post-immune suppression plasma.

immune suppression, the lymph node tissue viral species as compared to the plasma viral species had a significant increased level of average population diversity ($P < 0.001$) while also having a significant decreased level of average divergence from $EIAV_{PV}$ ($P < 0.001$). These data are consistent with the lymph node tissue serving as a reservoir of viral

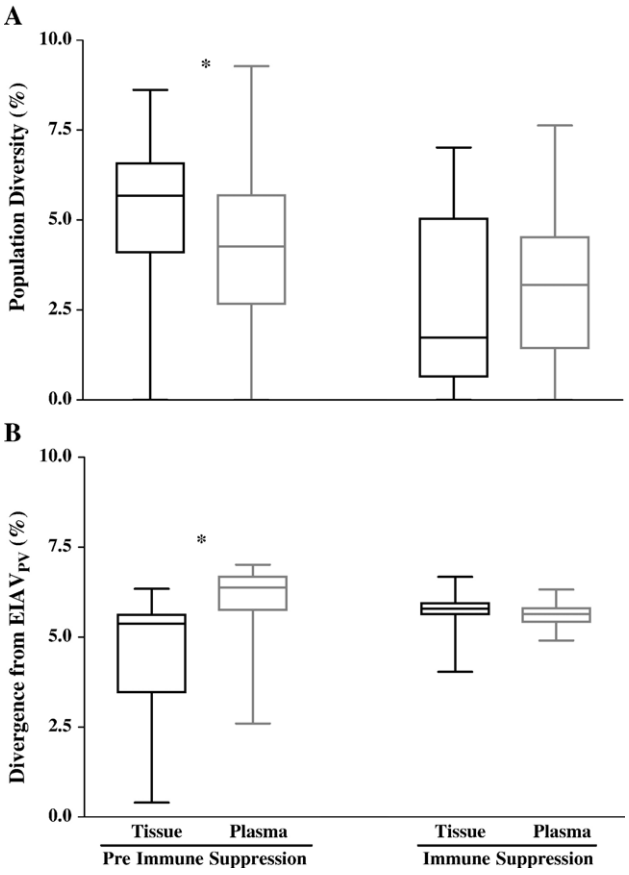

Fig. 4. Diversity and divergence comparisons between tissue and plasma virus species prior to and during immune suppression. The median (line) and quartile (box) differences between the tissue and plasma viral species nucleotide diversity (A) and divergence (B) are graphed for both the pre-immune suppression and post-immune suppression populations. Statistical significance of the differences between the tissue and plasma populations at each time point for each analyses was performed using nonparametric statistics, the Mann–Whitney test. *$P < 0.0001$.

populations. In contrast, during immune suppressive drug treatment, population diversity in the lymph node tissue was decreased as compared to the plasma population. Additionally, the lymph node species divergence from EIAV$_{PV}$ was slightly increased as compared to the plasma populations. These changes in diversity and divergence properties during immune suppression are inconsistent with the description of a reservoir sample and suggest that the drug treatment altered the status of the tissue by allowing free replication within and between microenvironments.

Determination of free flow of virus between tissues and plasma during immune suppression

To verify that we had overcome the barrier of tissue compartmentalization and established a free flow of virus between all tissue reservoirs and/or compartments, we performed various population analyses including phylogenetics, compartmentalization, and neutrality tests. If immune suppressive drug treatment allowed unrestricted viral replication and consequently free gene flow between tissue compartments and plasma, both compartmentalization and selection analyses should reveal the breakdown of the barriers that normally exist. The first tool we utilized was phylogenetics (Fig. 5A). A neighbor-joining phylogenetic tree was constructed utilizing nucleotide sequences from the plasma and tissue, prior to and during immune suppression, which had been aligned with and rooted to EIAV$_{PV}$. The majority of the quasispecies from both compartments and time points diverged from the same ancestral node of EIAV$_{PV}$ (Fig. 5A). The pre-immune suppression plasma and tissue species appeared compartmentalized, clustering tightly within their individual microenvironment populations, supported by high bootstrap values. Furthermore, while the quasispecies from the two compartments shared common ancestral nodes, they did not exhibit population intermingling within individual branches which is suggestive of compartmentalization. However, the isolates did not absolutely cluster as monophyletic groups. The pre-immune suppression tissue population contained 4 isolates which clustered close to EIAV$_{PV}$, indicative of archival sequences from early time points in the infection. These sequences will be discussed in detail when considering actual genomic evolution in the next section. In contrast to the pre-immune quasispecies, the post-immune suppression plasma and tissue species did not appear to be compartmentalized, demonstrating a high level of intermingling at multiple nodes that was indicative of freely merging species or a lack of compartmentalization.

To confirm the observations from the phylogenetic analysis, we performed a cladistic method of the Slatkin–Maddison test by analyzing the data set from both time points and compartments (Slatkin and Maddison, 1989, 1990). Phylogenetic trees were constructed from the pre-immune suppression and post-immune suppression populations individually prior to analysis in MacClade. We noted significant restricted gene flow in the pre-immune suppression populations ($P < 0.0001$), observing fewer numbers of steps to reconcile the real tree than in the random trees. However, during immune suppression, gene flow appeared unrestricted with the number of steps required to reconcile the real tree equivalent to that of the random trees. To support the observed trend of compartmentalization of viral quasispecies pre-immune suppression and the decay of compartmental barriers during immune suppression, we analyzed the level of gene flow as a measure of genetic diversity between the tissue and plasma at both time points (Fig. 5B). At the pre-immune suppression time point, the average level of gene flow (Nm value) between the tissue and plasma was 0.72, indicative of significant compartmentalization. In contrast, the post-immune suppression tissue and plasma Nm value was 26, demonstrating a complete lack of compartmentalization. As a final measure of the removal of immune restrictions to gene flow, we analyzed for the presence of positive selection between the tissue and the plasma prior to and during immune suppression (Fig. 5C). Positive selection ($\omega = 1.44$) was demonstrated prior to immune suppression; however, selection was neutral to weakly negative ($\omega = 0.97$) during immune suppression. These analyses all suggest that prior to immune suppression the viral populations in the tissue and plasma were restricted to their individual microenviron-

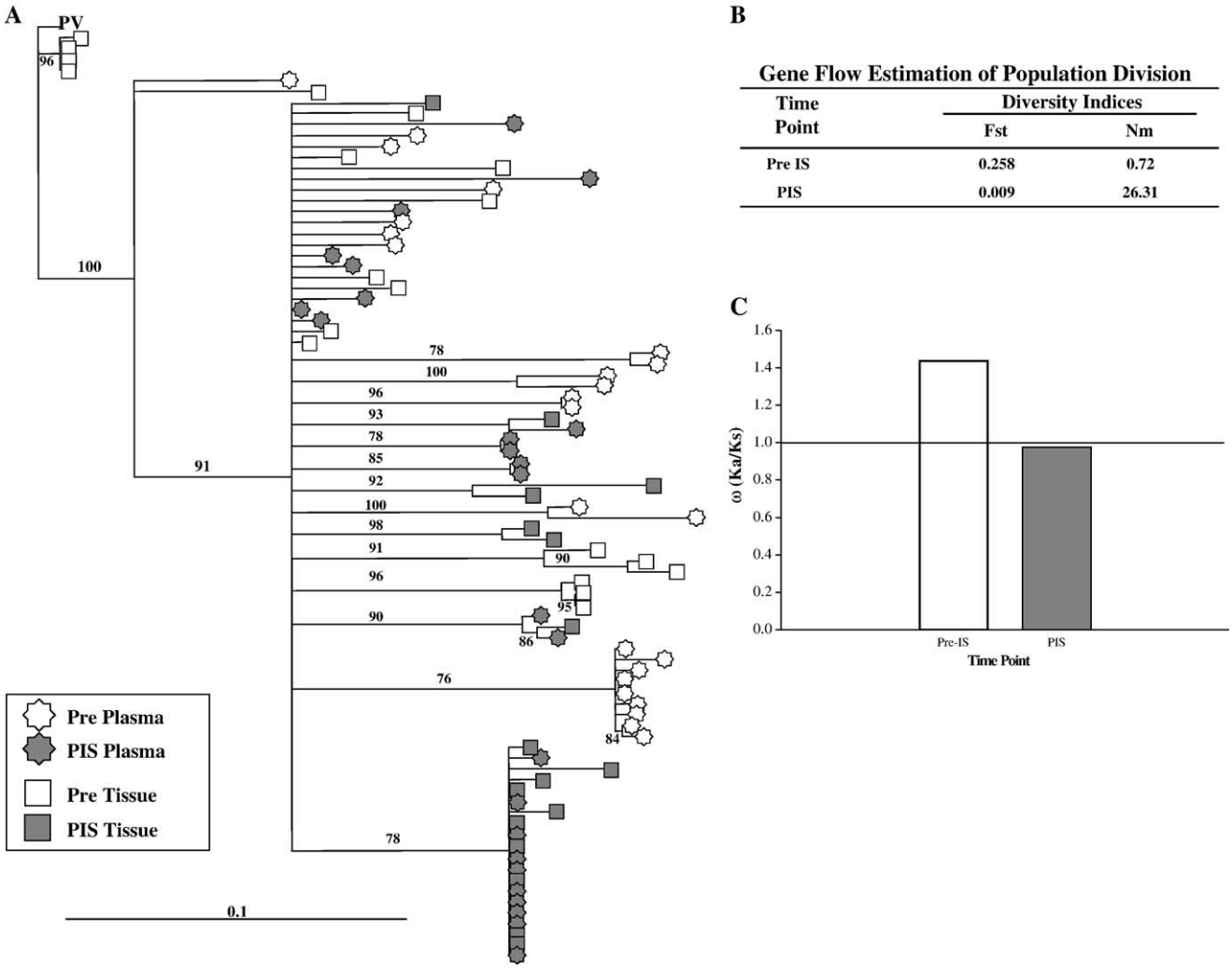

Fig. 5. Compartmental analyses of tissue and plasma virus populations prior to and during immune suppression. Compartmental integrity between the plasma and tissue populations was assessed through three separate analyses: (A) phylogenetics, (B) gene flow calculations, and (C) positive selection determinations. (A) A phylogenetic tree of aligned plasma and tissue immune suppression nucleotide sequences was constructed by the neighbor-joining method from Jukes Cantor corrected distances with the optimality criterion set to distance between pre-immune and post-immune suppression populations. The tree was rooted to $EIAV_{PV}$. Bootstrap values were determined over 1000 iterations and are indicated at the nodes of the branches. Branch lengths are proportional to the distance existing between the sequences. Pre, pre-immune suppression; PIS, post-immune suppression. (B) Estimates of gene flow were calculated using codon aligned nucleotide sequences and determined using software from DnaSP, V4.0 (Rozas et al., 2003; Rozas and Rozas, 1999). Fst and Nm were estimated according to Hudson et al. (1992). (C) Selection of viral populations was determined through calculations of the rates of synonymous (Ks) and nonsynonymous (Ka) nucleotide substitutions per site (Nielsen, 2001) of codon aligned nucleotide sequences. The ratio (ω) of Ks/Ka was evaluated using the programs available in DnaSP, v.4.0. The average number of nucleotide substitutions per site was determined between populations (compartments) with Jukes and Cantor corrections. Pre-IS, pre immune suppression; PIS, post-immune suppression. (—), indicates threshold of positive selection.

ments. However, upon immune suppressive drug treatment, the same analyses indicate that the normal barriers which restricted population replication dynamics were eliminated, and the quasispecies present in all compartments were estimated to be free flowing.

Evolutionary analyses of #567 viral quasispecies before and during immune suppression as compared to the viral species from disease episodes

To fully characterize the evolution of the viral populations in pony #567 and to quantify the relatedness of the immune suppression quasispecies to the preceding viral populations, the entire data set of pre-immune and post-immune suppression sequences from both compartments were aligned with the sequences from all 6 fever episodes and $EIAV_{PV}$ (Leroux et al., 2001). To directly examine evolutionary relationships, we constructed a neighbor-joining phylogenetic tree with bootstrap analysis using the aligned hand-edited nucleotide sequences encompassing the V3 to V7 variable regions of the gp90 *env* gene of the entire data set (Fig. 6A). The tree was rooted to the infecting inoculum, $EIAV_{PV}$. Examination of the data initially indicated that the majority of fever viral isolate clones clustered together separately by time point and that each febrile episode was followed by the emergence of a novel quasispecies that reflected mostly new isolates. Previously observed plasma viral

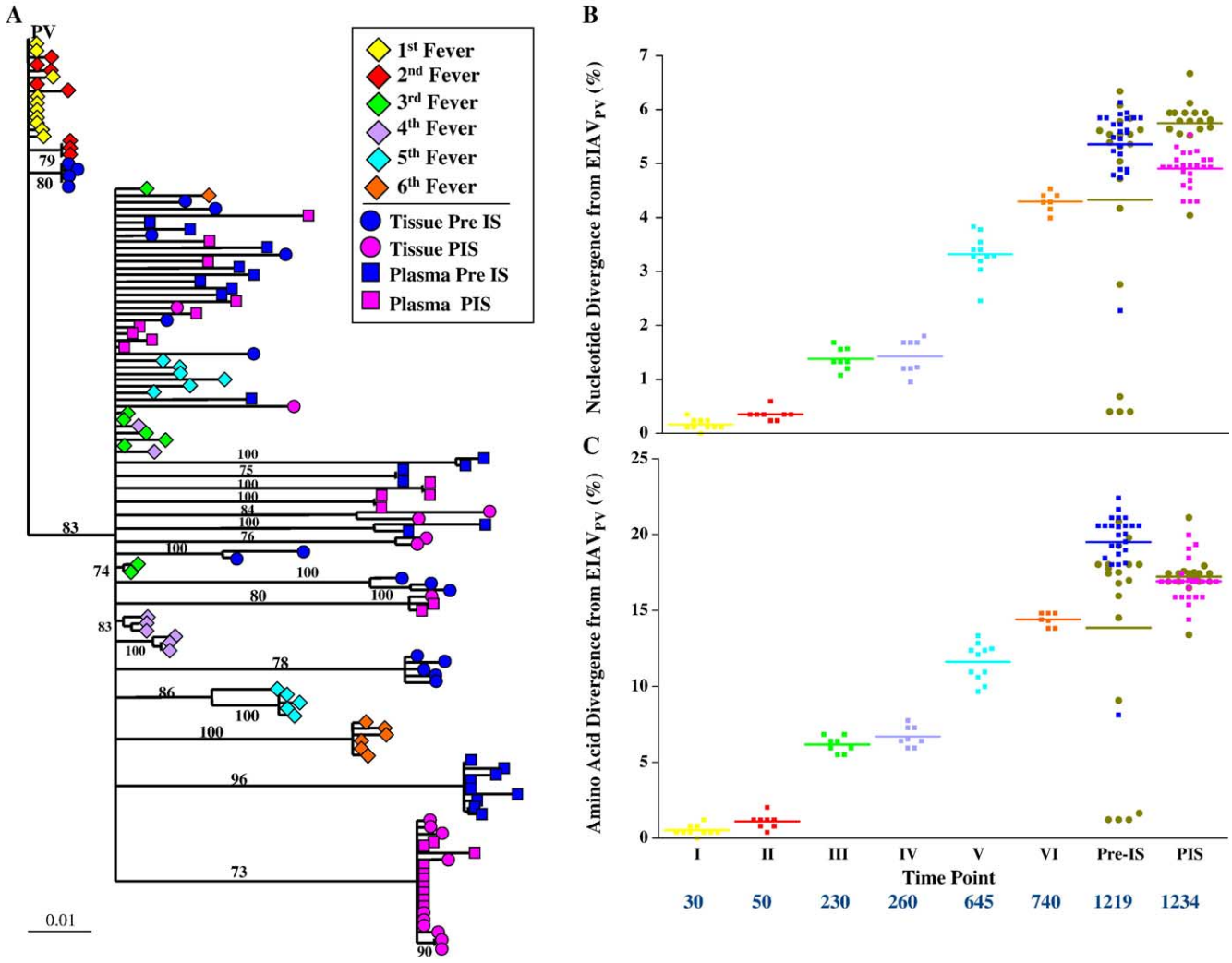

Fig. 6. Population comparisons of pony #567 from all stages of disease, including immune suppression. Evolutionary analyses of the immune suppression isolates were conducted. (A) A phylogenetic tree of aligned plasma and tissue immune suppression and febrile nucleotide sequences were constructed by the neighbor-joining method from Jukes Cantor corrected distances with the optimality criterion set to distance. The tree was rooted to $EIAV_{PV}$. Bootstrap values were determined over 1000 iterations and are indicated at the nodes of the branches. Branch lengths are proportional to the distance existing between the sequences. (B) Genetic distances of the nucleotide sequences were calculated using Distance software with Jukes Cantor correction (GCG). The distances of all sequenced clones were plotted as the divergence from the inoculating strain, $EIAV_{PV}$. The tissue population is represented by brown circles at the Pre-IS and PIS time points. (C) Genetic distances of the deduced amino acid sequences were calculated using Distance software with Jukes Cantor correction (GCG). The distances of all clones were plotted as the divergence from the inoculating strain, $EIAV_{PV}$. The tissue population is represented by brown circles at the Pre-IS and PIS time points. The days post-infection for both panels B and C are indicated below the *x* axis in blue, (—) represents mean divergence; I, II, III, IV, V, VI—fever episodes. Pre, pre-immune suppression; PIS, post-immune suppression.

variants were evidently eliminated with the cessation of a disease cycle, and a new population of viral variants was associated with the subsequent cycles of disease. The majority of pre-immune suppression plasma viral isolates followed a similar pattern, clustering together and at a distance from both $EIAV_{PV}$ and the febrile species in a manner suggestive of the emergence of novel quasispecies. This indicated that new viral species evolved during the inapparent stage of disease with no evidence of the preceding species. The greater part of the pre-immune suppression tissue isolates exhibited similar properties; however, there was less temporal structure as well as a grouping of archival sequences which clustered with close proximity to the second fever isolates. The majority of the post-immune suppression plasma viral variants were intermingled with the post-immune suppression tissue isolates and demonstrated similar clustering patterns as compared to the pre-immune suppression isolates but exhibited less overall distance from $EIAV_{PV}$. Additionally, the "ancestral" sequences which were present in the pre-immune suppression tissue were not reflected in the plasma or tissue of the viral isolates observed post-immune suppression. Moreover, the location of the immune suppression plasma and tissue quasispecies branchings did not indicate the presence of the original infectious inoculum or ancestral sequences previous to the third fever.

To specifically examine the degree of genetic distance of the immune suppression phase populations, we calculated the divergence of their nucleotide sequences from $EIAV_{PV}$ and plotted the data as a function of time (Fig. 6B). Divergence

from the inoculating strain increased over time, reaching 4.5% in the sixth fever population. Pre-immune suppression plasma isolates demonstrated increased divergence from the febrile variants at an average level of 5.75%. The pre-immune suppression tissue population appeared to have a lower divergence among its viral envelope species, averaging approximately 4.5% (although this number was lowered by a few isolates containing values less than 1.0%). Post-immune suppression plasma variants showed increased divergence as compared to the febrile isolates, but the average divergence was lower than that of the pre-immune isolates, averaging 5.25%, likely due to the free replication of minor, previously dominant species. Post-immune suppression tissue variants actually exhibited higher divergence, averaging 5.76%, as compared to the plasma variants which again reflected the free flow of virus between plasma and tissues during this period.

To determine whether these genotypic differences were also revealed as protein differences, we calculated the divergence of the deduced amino acid sequences of all viral quasispecies from $EIAV_{PV}$ (Fig. 6C). The pattern of increased divergence over time observed above was equally reflected in the quasispecies amino acid sequences. The average levels of amino acid divergence peaked in the pre-immune population at approximately 20%. The observed pattern of nucleotide and amino acid divergence among the disease and pre-immune suppression species indicated that the nucleotide changes were mostly nonsynonymous. In contrast, the post-immune suppression tissue variants amino acid sequences did not exhibit the increase in divergence observed in the nucleotide divergence, likely reflecting a loss of immune selection during the drug treatment. To confirm this observation, we examined population neutrality or selection through calculations of the rates of synonymous (Ks) and nonsynonymous (Ka) nucleotide substitutions per site between $EIAV_{PV}$ and all analyzed viral populations. The ratio (ω) of Ka/Ks was plotted as a function of time (Fig. 7). The first two fever quasispecies revealed ratios <1 reflecting negative selection or conservation, while all other time points exhibited ratios >1, indicating positive selection. Regardless of whether selection was positive or negative, a common pattern emerged in which immune selection increased over time throughout the chronic phase of disease, ω values increasing from 0.6 at the first fever to 2.5 during the sixth fever. The quasispecies from the pre- and post-immune suppression also demonstrated ratios indicative of positive selection (pre-immune suppression = 1.7, post-immune suppression = 1.5); however, it is noteworthy to mention that the level of selection appeared to decrease during the inapparent stage of disease when viral replication was in a state of immunological control.

Discussion

EIAV provides a uniquely dynamic model for investigating the natural immunologic control of lentiviral replication and disease and for elucidating the nature and role of genomic and antigenic variation in lentivirus persistence and pathogenesis. We, as well as others, have previously utilized this model for comprehensive studies of viral variation during persistent and inapparent infection. These studies have been limited primarily to the characterization of plasma virus quasispecies associated with sequential clinical episodes during chronic disease and variants that appear during inapparent disease. These analyses have revealed that a new population of quasispecies emerges

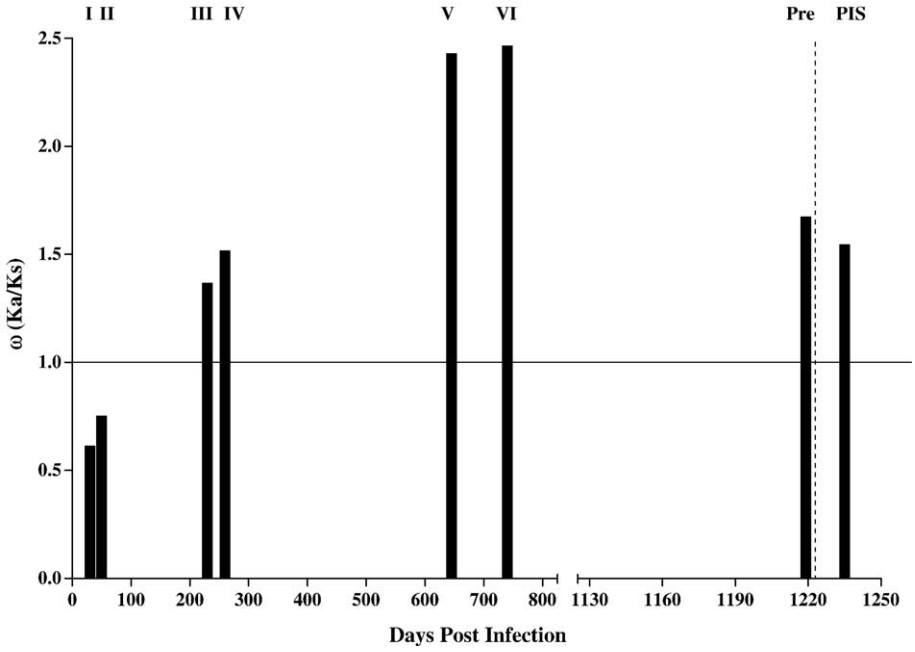

Fig. 7. Selection analyses of all populations from pony #567 as compared to $EIAV_{PV}$. Population neutrality or selection was determined through calculations of the rates of synonymous (Ks) and nonsynonymous (Ka) nucleotide substitutions per site (Nielsen, 2001). The ratio (ω) of Ks/Ka was evaluated using the programs available in DnaSP, v.4.0 and plotted as a function of time. I, II, III, IV, V, and VI indicate fever episodes. Pre, pre-immune suppression. PIS, post-immune suppression. (—), indicates threshold of positive selection. (---), indicates end of drug treatment.

with each new cycle of disease. Concomitant with the emergence of new populations is the apparent disappearance of preceding viral populations. We have previously shown that the initial infecting virus strain disappears in some instances as early as the second fever episode (within the first 2 months of infection) (Leroux et al., 2001). In fact, to date, there is no evidence as to the existence or status of the original virus strain in long-term lentiviral infections. Therefore, we endeavored here to ask whether this disappearance of ancestral species was due to elimination of the preceding quasispecies or to a tight containment of ancestral populations to tissue reservoirs.

EIAV persists in tissues and cells long after the signs of disease have subsided. Inapparent carriers of EIAV, as found with all persistent lentiviral infections, maintain reservoirs of viral infection for life. It is generally accepted that persistent viral infections, in contrast to acute viral infections, are lifelong infections that are never completely cleared by the host immune system. Long-term persistence in a host for certain viruses relies on the establishment of a true latency: a reversible, yet non-productive state of infection that involves the integration of the viral genome with the host genome and results in restricted gene expression or viral replication. Lentiviruses replicate continuously, even in the prolonged asymptomatic period for primate lentiviruses between primary infection and disease (HIV-1) or for EIAV in particular, during the final inapparent stage of disease (Leroux et al., 2001). HIV-1 has been demonstrated to persist in reservoirs consisting of small pools of latently infected resting memory CD4+ T cells carrying the integrated viral genome (Blankson et al., 2002; Chun et al., 1997). EIAV, however, naturally infects cells of the monocyte/macrophage lineage. Macrophage cells, unlike T cells, do not divide and are incapable of resuming a "resting state" as observed with infected CD4+ T cells. Ultimately, EIAV infection of macrophage culminates in a lytic infection, and therefore the viral genome is unlikely to reside in a state of "true" latency within these cells. Thus, long-term EIAV reservoirs likely exist as stable dynamic pools of infected cells undergoing low levels of viral replication in macrophage-rich tissues. The active replicating populations that have to this date been characterized focus on the "escape" populations that overtly circumvent the immune system well enough to replicate to levels that induce disease. The populations we were interested in elucidating were the minor species that may exist at very low levels, "hiding" from, or resistant to, the neutralizing antibodies and cellular immune responses elicited to these predecessor virus strains (Hammond et al., 2000; Howe et al., 2002; Leroux et al., 1997b). Therefore, we sought to induce active and increased replication of these species by removing the controlling factor of the equation, the immune system.

The desire to characterize the entire population present, minor species as well as dominant species dictated our decision to not perform limiting dilution for our PCR/cloning protocols (Rodrigo et al., 2001), while continuing to independently clone multiple reactions and select a high number of isolates. While the technique of limiting dilution is a very sound method for preventing the resampling of isolates, it also favors the cloning of dominant species, not minor ones which can be lost in the dilution process. Increasing the lower limit of the number of PCR reactions to clone as well as the lower limit of isolates to characterize not only increased our probability of sampling minor species, but also increased the number of unique clones we would characterize in terms of resampling (Rodrigo et al., 2001).

Dexamethasone suppression of the immune system has previously been demonstrated to suppress the overall immune system causing a recrudescence of viral replication and EIA disease in the majority of treated horses (Craigo et al., 2002; Kono et al., 1976; Tumas et al., 1994). We demonstrated here that the immune suppression of pony #567 was both successful and extensive (cf. Fig. 2), although clinical signs of disease did not accompany the treatment. Examination of the pre-immune and post-immune suppression viral quasispecies confirms what we have previously reported that, regardless of the low level of plasma virus replication, viral evolution is continuous. All of the pre-immune suppression plasma isolates demonstrated increased evolution and significant sequence divergence from the previously characterized febrile viral isolates (cf. Fig. 6B, 6th fever: pre-immune suppression plasma, $P = 0.0004$). The tissue reservoir prior to immune suppression did carry 4 isolate sequences which exhibited very little nucleotide divergence (less than 1.0%) from $EIAV_{PV}$ and clustered phylogenetically in close proximity to $EIAV_{PV}$. While initially these species appear to indicate the presence of ancestral sequences, the nucleotide sequences of the 4 species are quite different from those recorded from the fever episodes. Additionally, upon immune suppression, these variants apparently disappeared from the tissue and were also not evident in the post-immune suppression plasma. This suggests that these strains may express RNA but not produce replication-competent virus. Pre-immune suppression tissue variants also revealed divergent clones which demonstrated a similar level of divergence as fever five and six isolates. However, inspection of the specific residues indicated that these isolates were very different in sequence, even though they purely contained a similar level of divergence from $EIAV_{PV}$. Immune suppression induced increased viral replication and the circulation of previously uncharacterized quasispecies. Variants from this phase demonstrated a lower level of evolution phylogenetically, and the quasispecies primarily exhibited decreased divergence as compared to pre-immune suppression tissue and plasma isolates. However, as compared to the majority of previously cataloged species from the fever episodes, these latter species appeared to be primarily new quasispecies sequences, perhaps from a time point during the inapparent stage of disease that was uncharacterized. While pre-immune suppression tissue isolates and a number of post-immune suppression isolates indicated the presence of archival species, specific inspection of the deduced amino acid sequences revealed that all new populations, pre-immune and post-immune suppression-derived, were in fact distinct from previous populations. The few former species observed during immune suppression were from the pre-immune suppression isolates. The pre-immune and post-immune suppression variants were sampled approximately 2 weeks apart which may explain their overlapping V3 signatures.

All characterized populations prior to and during immune suppression revealed mostly nonsynonymous mutations, indicative of ongoing evolution. Furthermore, immune selection analyses indicated that all populations were under positive selection after the second fever episode. Interestingly, selection increased sequentially during the chronic stage of disease paralleling the increase in the variation of the virus. Selection slightly declined in the inapparent stage which was likely due to the decreased interaction of new viral variants with the immune system. However, the immune suppressive drug treatment likely accounted for the slight decrease in positive selection between the pre-immune and immune suppression time points.

The fact that the divergence from $EIAV_{PV}$ was reduced in the post-immune suppression plasma as compared to the pre-immune suppression isolates suggests that, while these isolates were previously uncharacterized, they most likely arose sometime after the sixth fever episode during the inapparent stage of disease. Ultimately, all archival sequences failed to align with the inoculating viral strain or the early species found in the fever episodes. Therefore, the results of this investigation indicate that the original infectious viral strain, as well as the majority of early viral quasispecies, was undetectable or evidently eliminated by the immune system of the host during persistent EIAV infection.

Eradication of lentiviral populations is impeded by the remarkable persistence and pathogenesis associated with these viral infections. A primary mechanism of lentiviral persistence is the ability of the viruses to evolve in response to biological and immunological selective pressures with an extraordinary array of genetic and antigenic variations. Further means of persistence also involve the establishment of latent viral reservoirs. We have for the first time demonstrated that the equine immune system appears to achieve an effective elimination of the original infectious virus as well as the early circulating viral quasispecies that arise through evolution. Characterization of the EIAV immune suppression period populations revealed mostly novel quasispecies which were distinct from previously characterized populations from all stages of disease. As shown by the EIAV system, immune control against viral replication can be efficiently established to successfully restrain emerging viral populations. In EIAV-infected ponies, host immune responses have matured to the point that virus variation occurs, but new populations are unable to escape established immune control. Ultimately, the host immune system is able to effectively eliminate a diverse array of antigenic variants; yet, viral persistence is maintained by the relentless evolution of new envelope populations from tissue reservoirs in response to ongoing immune pressures.

Materials and methods

Experimental infection, clinical evaluation and sample collection

An outbred mixed-breed pony (#567) was experimentally inoculated intravenously with 10^3 $TCID_{50}$ of the pathogenic strain $EIAV_{PV}$. The clinical and immune responses of this experimentally infected pony during chronic and inapparent infection have been extensively described (Hammond et al., 1997, 2000; Leroux et al., 1997b, 2001). Rectal temperatures and clinical status were recorded daily. Clinical EIA episodes were determined on the basis of rectal temperature and platelet count in combination with the presence of infectious plasma virus (Leroux et al., 1997b; Lichtenstein et al., 1996; Montelaro et al., 1993). Whole blood samples were fractionated for enumeration of platelets (Unopette microcollection system, Becton-Dickinson, Rutherford, NJ). Plasma samples were collected during each disease cycle (defined as rectal temperature >39 °C and platelet number <100,000/μl of whole blood) and daily during immune suppression and stored at −80 °C until RNA extraction was performed.

Immune suppression

Procedures for immune suppression of the EIAV-infected pony were based on protocols implemented previously (Craigo et al., 2002) and based on published protocols of Kono et al. (1976) and Tumas et al. (1994). Briefly, dexamethasone (Phoenix Science, Kansas City, MO) was administered at a dose of 0.11 mg/kg body weight/day, intramuscularly for 14 days. The pony was monitored daily by complete blood count (CBC).

Monitoring of immune suppression by DTH and FACS analysis

Skin tests for delayed-type hypersensitivity (Baus et al., 1996; Hodgin et al., 1978) reactions were performed during the pre-immune suppression, immune suppression, and post-immune suppression periods. Skin test sites were prepared by shaving and cleaning small areas on the neck. The pony was intradermally administered (at different sites on the neck) both 50 μg of PHA (Sigma, St. Louis, MO) in 1 ml of saline and 1 ml of saline alone. The net increase in skin thickness was determined from measurements made with constant tension calipers 24 h post-injection of antigen. DTH ratios were calculated as the ratio of antigen (PHA) reaction to control (saline) reaction. Flow cytometric analyses of equine cell surface antigens were conducted as previously described (Hammond et al., 1999). Equine-specific monoclonal antibodies (mAb) used to quantitate levels of specific cell surface antigens were as follows: CD4 (mAb HB61A; VMRD, Inc., Pullman, WA), CD8 (mAb HT14A; VMRD, Inc., Pullman, WA), and IgG_1 (mAb CVS1; Serotec, Raleigh, NC).

RNA Purification and RT-PCR

Viral RNA was extracted from plasma and submandibular lymph node tissue samples prior to and during immune suppression as previously described (Craigo et al., 2002; Harrold et al., 2000; Leroux et al., 1997b, 2001). Reverse transcription of 2 to 5 μl of purified viral RNA was performed with the SuperScriptII PreAmplification System (GibcoBRL, Rockville, MD) as specified by the manufacturer using the EIAV-specific primer PV12AS (Leroux et al., 1997b). Multiple

nested amplifications of the gp90 envelope gene were performed as previously described (Leroux et al., 2001) using the Elongase mix (Gibco BRL, Rockville, MD) and 5 μl of the cDNA in a final volume of 50 μl.

Quantitation of virus RNA levels in plasma

Semiquantitative measurements of copies of viral genomic RNA molecules per milliliter of plasma were determined in an RT-PCR-based assay as described previously (Hammond et al., 2000).

Cloning and sequencing of RT-PCR products

Several independent RT-PCR products (at least 3 independent RT reactions and 6 to 8 independent nested PCR reactions) were generated from plasma and tissue samples taken before or during immune suppression, gel-purified using Qiagen's Qiaex Gel Purification System (Valencia, CA) and cloned individually into the pCR2.1-TOPO vector from the TOPO TA Cloning kit (Invitrogen, Carlsbad, CA). Due to the highly unstable nature of EIAV *env* sequences when associated with high copy plasmids, ligations were transformed in Stbl2 cells (Invitrogen, Carlsbad, CA). Clones were screened for the proper size insert by PCR using M13 primers from the TOPO TA Cloning kit. Plasmid DNA was extracted and purified with a midiprep kit (Qiagen, Valencia, CA). Clones (17–25 from each sample) were automatically sequenced with the Taq Dye Deoxy Terminator Cycle Sequencer Kit (Applied Biosystems, Foster City, CA) using internal EIAV primers (variable region 3 through variable region 7) as previously described (Leroux et al., 1997b). DNA sequences were resolved with an ABI Prism 373 DNA sequencer (Applied Biosystems, Foster City, CA). Error rate associated with our nested amplification with the SuperScript and Elongase polymerases was previously determined to be 0.015% (3 substitutions per 19,510 bp sequenced) (Leroux et al., 1997b).

Sequence and population analyses

Sequences were assembled and error checked using GeneJockey II (Biosoft, Cambridge, UK). Nucleotide and deduced amino acid sequences from each clone were aligned using the ClustalW multiple sequence alignment program from the GCG Wisconsin software package (Genetics Computer Group, 2003) and edited manually and codon aligned when necessary. The sequences were aligned using the PAM 250 (Dayhoff et al., 1978) matrix and an open and extend gap penalty cost of 8 and 12 respectively. Genetic algorithm settings were based on the default parameters. Divergence/diversity analyses were determined utilizing Jukes Cantor population distance calculations for nucleotide sequences as executed in the program Distance from the GCG package of software. Statistical significances of the mean genetic distances between plasma and tissue samples were evaluated using a Mann–Whitney two-tailed test, implemented in GraphPad InStat version 3.00 (GraphPad Software, San Diego California USA, www.graphpad.com).

Phylogenetic trees of aligned sequences were constructed by the neighbor-joining method of Jukes Cantor corrected distances with the optimality criterion set to distance as measured in PAUP (Swofford, 2001). Statistical significance of branchings and clustering was assessed by bootstrap resampling of 1000 pseudoreplicates on the complete data set; trees were rooted to the original infectious inoculum, $EIAV_{PV}$. The trees were edited for publication using Treeview68K version 1.5 (Page, 1996).

Compartmental relationships of the viral samples were determined using a cladistic method of the Slatkin–Maddison test (Poss et al., 1998; Slatkin and Maddison, 1989, 1990) by analyzing the entire data set (prior to and during immune suppression) from both compartments, tissue and blood. A UPGMA phylogenetic tree was constructed for sequences from both the plasma and tissue from both time points analyzed individually. A multiple state character was created such that sequences were assigned the same state based on what compartment they originated from. The number of changes or evolutionary steps required to reconcile the new individual states to the phylogenetic true tree was computed using MacClade 3.06 (Maddison and Maddison, 1992) assuming both soft and hard polytomies (Beerli et al., 2001; Maddison and Maddison, 1992). If all sequences in a compartment were monophyletic, the maximum number of character state changes would equal the number of compartments minus one. If the sequences were not compartmentalized, the number of changes would increase. Statistical significance of the estimated migration events being significantly smaller than expected by chance in a non-compartmentalized population was determined by constructing 10,000 random trees made by random joining/splitting of the phylogenetic tree constructed for each data set. If there was compartmentalization, the number of steps from the realized tree would be fewer than the random trees. Compartmentalization was considered statistically significant if fewer steps were seen in the true tree than in 95% of the random trees (Beerli et al., 2001).

Standard population genetic parameters for DNA diversity were estimated using DnaSP, V4.0 (Rozas et al., 2003; Rozas and Rozas, 1999). Genetic differentiation between populations was assessed by estimating Fst, the fraction of nucleotide diversity as a result of genetic variation between populations (Hudson et al., 1992). The significance of Fst was determined by sampling the data 1000 times. The average level of gene flow, Nm, between the different populations was determined from Fst (Hudson et al., 1992; Neigel, 1997). A value of Nm equal or less than one indicated significant population subdivision.

Population neutrality or selection was determined through calculations of the rates of synonymous (Ks) and nonsynonymous (Ka) nucleotide substitutions per site (Nielsen, 2001). The ratio (ω) of Ka/Ks was evaluated using the programs available in DnaSP, v.4.0 (Rozas et al., 2003; Rozas and Rozas, 1999). The average number of nucleotide substitutions per site was determined within populations and between populations (and/or compartments) with Jukes and Cantor correction (between populations, Dxy, equation 10.20; between species, K; equation 5.3, but computing as the average of all comparisons

between populations; Nei, 1987). Estimation separately for synonymous and nonsynonymous sites is performed using Nei and Gojobori equations 1–3 (Nei and Gojobori, 1986). Results were assessed as follows: negative selection or conservation ($\omega < 1$); neutral evolution ($\omega = 1$); positive selection for change or increased viral replication ($\omega > 1$).

Nucleotide sequence accession numbers

The newly analyzed sequences were submitted to GenBank and have been assigned accession numbers AY858699–AY858784.

Acknowledgments

We thank John Cardamone for his excellent technical assistance in DNA sequencing, and Gary Thomas and Brian Meade for animal care. The authors would also like to thank Jonathan D. Steckbeck for editing the manuscript. This work was supported by the National Institutes of Health grant number R01 AI 25850, by funds from the Lucille P. Markey Charitable Trust and the Kentucky Agricultural Experimental Station, and by a grant from the Pittsburgh Supercomputing Center through the NIH National Center for Research Resources, resource grant 2 P41 RR06009.

References

Bakhanashvili, M., Hizi, A., 1993. Fidelity of DNA synthesis exhibited in vitro by the reverse transcriptase of the lentivirus equine infectious anemia virus. Biochemistry 32, 7559–7567.

Baus, E., Andris, F., Dubois, P.M., Urbain, J., Leo, O., 1996. Dexamethasone inhibits the early steps of antigen receptor signaling in activated T lymphocytes. J. Immunol. 156, 4555–4561.

Beerli, P., Grassly, N.C., Kuhner, M.K., Nickle, D., Pybus, O., Rain, M., Rambaut, A., Rodrigo, A.G., Wang, Y., 2001. Population genetics of HIV: Parameter estimation using geneaology-based methods. In: Rodrigo, A.G., Learn, G.H. (Eds.), Computational and Evolutionary Analyses of HIV Sequences. Kluwer Academic Publication, Boston, pp. 217–252.

Blankson, J.N., Persaud, D., Siliciano, R.F., 2002. The challenge of viral reservoirs in HIV-1 infection. Annu. Rev. Med. 53, 557–593.

Chun, T.W., Carruth, L., Finzi, D., Shen, X., DiGiuseppe, J.A., Taylor, H., Hermankova, M., Chadwick, K., Margolick, J., Quinn, T.C., Kuo, Y.H., Brookmeyer, R., Zeiger, M.A., Barditch-Crovo, P., Siliciano, R.F., 1997. Quantification of latent tissue reservoirs and total body viral load in HIV-1 infection. Nature 387, 183–188.

Clements, J.E., Zink, M.C., Narayan, O., Gabuzda, D., 1994. Lentivirus infection of macrophages. Immunol. Ser. 60, 589–600.

Craigo, J.K., Leroux, C., Howe, L., Steckbeck, J.D., Cook, S.J., Issel, C.J., Montelaro, R.C., 2002. Transient immune suppression of inapparent carriers infected with a principal neutralizing domain-deficient equine infectious anaemia virus induces neutralizing antibodies and lowers steady-state virus replication. J. Gen. Virol. 83, 1353–1359.

Dayhoff, M.O., Schwartz, R.M., Orcutt, B.C., 1978. A model of evolutionary change in proteins. matrices for detecting distant relationships. In: Dayhoff, M.O. (Ed.), Atlas of Protein Sequence and Structure, vol. 5. National Biomedical Research Foundation, Washington, DC, pp. 345–358.

Finzi, D., Blankson, J., Siliciano, J.D., Margolick, J.B., Chadwick, K., Pierson, T., Smith, K., Lisziewicz, J., Lori, F., Flexner, C., Quinn, T.C., Chaisson, R.E., Rosenberg, E.S., Walker, B., Gange, S., Gallant, J., Siliciano, R.F., 1999. Latent infection of CD4+ T cells provides a mechanism for lifelong persistence of HIV-1, even in patients on effective combination therapy. Nat. Med. 5, 512–517.

Genetics Computer Group, 2003. Program Manual for the Wisconsin Package. Genetics Computer Group, Madison, WI.

Greene, W.K., Meers, J., del Fierro, G., Carnegie, P.R., Robinson, W.F., 1993. Extensive sequence variation of feline immunodeficiency virus env genes in isolates from naturally infected cats. Arch. Virol. 133, 51–62.

Hammond, S.A., Cook, S.J., Lichtenstein, D.L., Issel, C.J., Montelaro, R.C., 1997. Maturation of the cellular and humoral immune responses to persistent infection in horses by equine infectious anemia virus is a complex and lengthy process. J. Virol. 71, 3840–3852.

Hammond, S.A., Horohov, D., Montelaro, R.C., 1999. Functional characterization of equine dendritic cells propagated ex vivo using recombinant human GM-CSF and recombinant equine IL-4. Vet. Immunol. Immunopathol. 71, 197–214.

Hammond, S.A., Li, F., McKeon Sr., B.M., Cook, S.J., Issel, C.J., Montelaro, R.C., 2000. Immune responses and viral replication in long-term inapparent carrier ponies inoculated with equine infectious anemia virus. J. Virol. 74, 5968–5981.

Han, Y., Lassen, K., Monie, D., Sedaghat, A.R., Shimoji, S., Liu, X., Pierson, T.C., Margolick, J.B., Siliciano, R.F., Siliciano, J.D., 2004. Resting CD4+ T cells from human immunodeficiency virus type 1 (HIV-1)-infected individuals carry integrated HIV-1 genomes within actively transcribed host genes. J. Virol. 78, 6122–6133.

Harrold, S.M., Cook, S.J., Cook, R.F., Rushlow, K.E., Issel, C.J., Montelaro, R.C., 2000. Tissue sites of persistent infection and active replication of equine infectious anemia virus during acute disease and asymptomatic infection in experimentally infected equids. J. Virol. 74, 3112–3121.

Hodgin, E.C., McGuire, T.C., Perryman, L.E., Grant, B.D., 1978. Evaluation of delayed hypersensitivity responses in normal horses and immunodeficient foals. Am. J. Vet. Res. 39, 1161–1167.

Howe, L., Leroux, C., Issel, C.J., Montelaro, R.C., 2002. Equine infectious anemia virus envelope evolution in vivo during persistent infection progressively increases resistance to in vitro serum antibody neutralization as a dominant phenotype. J. Virol. 76, 10588.

Hudson, R.R., Slatkin, M., Maddison, W.P., 1992. Estimation of levels of gene flow from DNA sequence data. Genetics 132, 583–589.

Kono, Y., Hirasawa, K., Fukunaga, Y., Taniguchi, T., 1976. Recrudesence of equine infectious anemia by treatment with immunosuppressive drugs. Natl. Inst. Anim. Health Q. 16, 8–15.

Lassen, K.G., Bailey, J.R., Siliciano, R.F., 2004. Analysis of human immunodeficiency virus type 1 transcriptional elongation in resting CD4+ T cells in vivo. J. Virol. 78, 9105–9114.

Leroux, C., Chastang, J., Greenland, T., Mornex, J.F., 1997a. Genomic heterogeneity of small ruminant lentiviruses: existence of heterogeneous populations in sheep and of the same lentiviral genotypes in sheep and goats. Arch. Virol. 142, 1125–1137.

Leroux, C., Issel, C., Montelaro, R.C., 1997b. Novel and dynamic evolution of equine infectious anemia virus genomic quasispecies associated with sequential disease cycles in an experimentally infected pony. J. Virol. 71, 9627–9639.

Leroux, C., Craigo, J.K., Issel, C.J., Montelaro, R.C., 2001. Equine infectious anemia virus genomic evolution in progressor and nonprogressor ponies. J. Virol. 75, 4570–4583.

Lichtenstein, D.L., Issel, C.J., Montelaro, R.C., 1996. Genomic quasispecies associated with the initiation of infection and disease in ponies experimentally infected with equine infectious anemia virus. J. Virol. 70, 3346–3354.

Maddison, W.P., Maddison, D.R., 1992. MacClade: Analysis of Phylogeny and Character Evolution, 3rd ed. Sinauer Associates, Sunderlan, MA.

Montelaro, R., Ball, J.M., Rushlow, K., 1993. Equine retroviruses. In: Levy, J.A. (Ed.), The Retroviridae. Plenum Press, New York, pp. 257–360.

Nei, M., 1987. Molecular Evolutionary Genetics. Columbia Univ. Press, New York.

Nei, M., Gojobori, T., 1986. Simple methods for estimating the numbers of synonymous and nonsynonymous nucleotide substitutions. Mol. Biol. Evol. 3, 418–426.

Neigel, J.E., 1997. A comparison of alternative strategies for estimating gene flow from genetic markers. Annu. Rev. Ecol. Syst. 28, 105–128.

Nickle, D.C., Jensen, M.A., Shriner, D., Brodie, S.J., Frenkel, L.M., Mittler, J.E., Mullins, J.I., 2003a. Evolutionary indicators of human immunodeficiency virus type 1 reservoirs and compartments. J. Virol. 77, 5540.

Nickle, D.C., Shriner, D., Mittler, J.E., Frenkel, L.M., Mullins, J.I., 2003b. Importance and detection of virus reservoirs and compartments of HIV infection. Curr. Opin. Microbiol. 6, 410–416.

Nielsen, R., 2001. Detecting selection in protein coding genes using the rate of nonsynonymnous and synonymous divergence. In: Rodrigo, A.G. (Ed.), Computational and Evolutionary Analyses of HIV Sequences. Kluwer Academic Publication, Boston, pp. 253–267.

Oaks, J.L., McGuire, T.C., Ulibarri, C., Crawford, T., 1998. Equine infectious anemia virus is found in tissue macrophages during subclinical infection. J. Virol. 72, 7263–7269.

Page, R.D.W., 1996. TREEVIEW: an application to display phylogenetic trees on personal computers. Comput. Appl. Biosci. 12, 357–358.

Payne, S.L., Salinovich, O., Nauman, S.M., Issel, C.J., Montelaro, R.C., 1987. Course and extent of variation of equine infectious anemia virus during parallel persistent infections. J. Virol. 61, 1266–1270.

Payne, S.L., Rushlow, K., Dhruva, B.R., Issel, C.J., Montelaro, R.C., 1989. Localization of conserved and variable antigenic domains of equine infectious anemia virus envelope glycoproteins using recombinant env-encoded protein fragments produced in *Escherichia coli*. Virology 172, 609–615.

Persaud, D., Zhou, Y., Siliciano, J.M., Siliciano, R.F., 2003. Latency in human immunodeficiency virus type 1 infection: no easy answers. J. Virol. 77, 1659.

Poss, M., Rodrigo, A.G., Gosink, J.J., Learn, G.H., de Vange, P.D., Martin Jr., H.L., Bwayo, J., Kreiss, J.K., Overbaugh, J., 1998. Evolution of envelope sequences from the genital tract and peripheral blood of women infected with clade A human immunodeficiency virus type 1. J. Virol. 72, 8240–8251.

Preston, B.D., Poiesz, B.J., Loeb, L.A., 1988. Fidelity of HIV-1 reverse transcriptase. Science 242, 1168–1171.

Roberts, J.D., Bebenek, K., Kunkel, T.A., 1988. The accuracy of reverse transcriptase from HIV-1. Science 242, 1171–1173.

Rodrigo, A.G., Hanley, E.W., Goracke, P.C., Learn, G.H., 2001. Sampling and processing HIV molecular sequences: a computational evolutionary biologist's perspective. In: Rodrigo, A.G., Learn, G.H. (Eds.), Computational and Evolutionary Analysis of HIV Molecular Sequences. Kluwer Academic Publishers, Norwell, MA, pp. 1–18.

Rozas, J., Rozas, R., 1999. DnaSP version 3: an integrated program for molecular population genetics and molecular evolution analysis. Bioinformatics 15, 174–175.

Rozas, J., Sanchez-DelBarrio, J.C., Messeguer, X., Rozas, R., 2003. DnaSP, DNA polymorphism analyses by the coalescent and other methods. Bioinformatics 19, 2496–2497.

Simmonds, P., Balfe, P., Ludlam, J., Bishop, O., Brown, A.J., 1990. Analysis of sequence diversity in hypervariable regions of the external glycoprotein of human immunodeficiency virus type 1. J. Virol. 64, 5840–5850.

Slatkin, M., Maddison, W.P., 1989. A cladistic measure of gene flow inferred from the phylogenies of alleles. Genetics 123, 603–613.

Slatkin, M., Maddison, W.P., 1990. Detecting isolation by distance using phylogenies of genes. Genetics 126, 249–260.

Starcich, E.S., Hahn, B.H., Shaw, G.M., McNeely, P.D., Modrow, S., Wolf, H., Parks, E.S., Parks, W.P., Josephs, S.F., Gallo, R.C., 1986. Identification and characterization of conserved and variable regions in the envelope gene of HTLV-III/LAV, the retrovirus of AIDS. Cell 45, 637–648.

Suarez, D.L., Whetstone, C.A., 1995. Identification of hypervariable and conserved regions in the surface envelope gene in the bovine lentivirus. Virology 212, 728–733.

Swofford, D.L., 2001. PAUP: Phylogenetic Analysis Using Parsimony and Other Methods. Sinauer Associates, Sunderlan, MA.

Tumas, D.B., Hines, M.T., Perryman, L.E., Davis, W.C., McGuire, T.C., 1994. Corticosteroid immunosuppression and monoclonal antibody-mediated CD5+ T lymphocyte depletion in normal and equine infectious anemia virus-carrier horses. J. Gen. Virol. 75, 959–968.

Zheng, Y.H., Nakaya, T., Sentsui, H., Kameoka, M., Kishi, M., Hagiwara, K., Takahashi, H., Kono, Y., Ikuta, K., 1997a. Insertions, duplications and substitutions in restricted gp90 regions of equine infectious anemia virus during febrile episodes in an experimentally infected horse. J. Gen. Virol. 78, 807–820.

Zheng, Y.H., Sentsui, H., Nakaya, T., Kono, Y., Ikuta, K., 1997b. In vivo dynamics of equine infectious anemia viruses emerging during febrile episodes: insertions/duplications at the principal neutralizing domain. J. Virol. 71, 5031–5039.